Fachtagung "Experimentelle Strömungsmechanik"
6.–8. September 2022, Ilmenau

Untersuchung der Ausströmungshomogenität einer klimatisierten Matratze

Investigation of the airflow homogeneity of an air-conditioning mattress

Michael Mommert[1], Robert Brinkema[1], Andreas Westhoff[1], Till Fischbach[2]
[1] DLR - Insitute of Aerodynamics and Flow Technologies - Ground Vehicles, Bunsenstraße 10, 37073 Göttingen
[2] Comlogo GmbH, Allerbachstr. 29, 37586 Dassel

Klimatisierung, Matratze, PIV, Transitzeitmethode
air-conditioning, mattress, PIV, transit time method

Abstract

Air-conditioning mattresses are used in the treatment of sleep disorders, as temperature and humidity discomfort are among the most common complaints of those affected. In the development of a new type of air-conditioned mattress with an integrated control function, the aim is to achieve a homogeneously distributed air outflow to ensure a cooling effect with simultaneous removal of the humidity caused by sweating. This paper describes the experimental approach for the optical measurement of the air velocity above the surface of the mattress. For the evaluation of the raw images, a transit-time method is presented as an alternative to the conventional stereoscopic Particle Image Velocimetry (stereo PIV). The results of both methods are discussed to analyze the air flow of the mattress.

Introduction

According to a survey by a health insurance company (see Techniker Krankenkasse 2017), 40 % of German's population state that their sleep is frequently impaired by the room climate that is too hot or too cold. Mattresses with an integrated air-conditioning offer a solution for better sleeping comfort. They provide both a heating and a cooling function, of which the latter is achieved through the evaporation of sweat. To ensure that the evaporation occurs regardless of the sleeping position, a homogeneous airflow distribution throughout the entire upper surface of the mattress (see Fig. 1 for structure) is required. Further clinical applications of air-conditioning mattresses to alleviate nocturnal hyperhidrosis also depend on this property.
Therefore, the analysis of the homogeneity of the airflow is an important step in the development of a novel air-conditioning mattress.

Experimental setup

As the expected flow velocities range below 0.01 m/s, thermal or sonar velocity probes are not suitable to resolve the flow field. Therefore, an optical, particle-based measurement technique was applied. Moreover, controlled ambient conditions were needed to avoid interfering secondary flows. For this, the mattress (900 mm x 2000 mm) was placed in a climate chamber at well-defined conditions.

GALA e.V., Karlsruhe, Germany, ISBN 978-3-9816764-8-8

Figure 1 shows a schematic sketch of the setup. For the illumination, an Innolas Spitlight 600 Nd:YAG laser with a pulse frequency of 10 Hz was used to generate a horizontal light sheet parallel to the top surface of the mattress. This 5 mm thick light sheet was positioned in different heights h_{LS} = {17 mm, 41 mm}, with 17 mm being the lowest possible setting to avoid excessive reflections of the scattered laser light by the mattress.
To provide the flow with tracer particles, di-ethyl-hexyl sebacate (DEHS) aerosol was introduced into the climate chamber. The utilized Laskin-nozzle based seeding generator typically produces a droplet size distribution with a mean diameter of around 1 µm (see Raffel et al. 2018). This small size allows the particles to be drawn into the mattress through the ventilation unit at the foot end and to be transported through the channels and foam of the mattress.

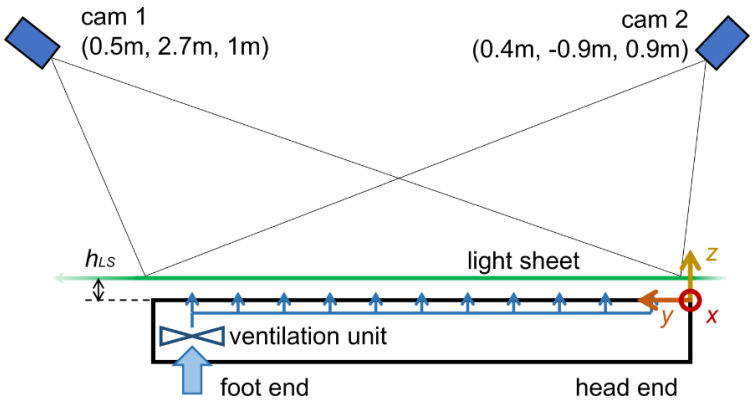

Fig. 1: Sketch of the optical measurement setup to measure the homogeneity of the airflow through the mattress (blue arrows).

The light scattering of the DEHS droplets was recorded by two pco.4000 cameras equipped with Zeiss 21mm *f*/2.8 Milvus (camera 1) or Distagon T* (camera 2) lenses via Scheimpflug mounting adaptors. Due to the field curvature of these wide-angle lenses, apertures of *f*/8 (camera 1) and *f*/11 (camera 2) were set to achieve sharpness over complete length of the mattress for the respective cameras.

Assessment of raw images

Caused by the required wide fields of view, the resolution of the cameras and their small aperture setting, single particles were barely detectable on the raw images as shown in the first time frame of Fig. 2. This low sharpness is especially present on camera 2, whose viewing angle fell within the range of less intense backscatter.
However, with the activation of the ventilation device, darker structures become visible in the light sheet plane. This effect is depicted in Fig. 2, which shows the image time series for both cameras for a measurement case of the 100 % pulse width modulation (PWM) setting of the ventilation unit. The first frames of these series represent a state, in which the DEHS aerosol within the climate chamber is illuminated by the light sheet. In the subsequent frames, dark regions appear within the light sheet starting from the foot end. These dark regions are caused by a reduction of seeding density of the air resting within the mattress due to settling. In the following, the regions spread throughout the mattress until the aerosol-rich air which was freshly drawn into and transported through the mattress reaches the light sheet and displaces the darker areas again.
This behavior allows the velocity evaluations which do not rely on the resolution of single particles which are explained in more detail in the next two sections.

GALA e.V., Karlsruhe, Germany, ISBN 978-3-9816764-8-8

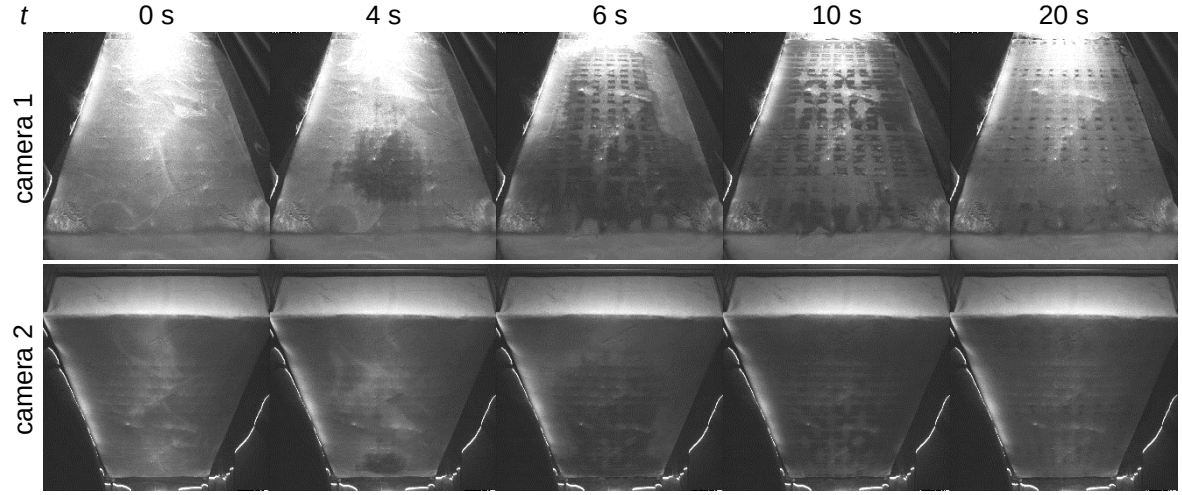

Fig. 2: Series of exemplary raw images (h_{LS} = 17 mm) for camera 1 (top) and camera 2 (bottom) starting with switching on the ventilation device at t = 0 s.

PIV evaluation

Aerosol concentration gradients were used to correlate in the PIV algorithm because the boundaries of the bright aerosol-rich and dark aerosol-free regions should shift similarly to individual particles. For this purpose, the start of the PIV measurement and the ventilation unit were synchronized as these swathe structures consistently emerged when the ventilation unit was started after a shut-down period of approximately 2 minutes. The parameters of these stereo PIV evaluations are listed in Tab. 1.

Tab. 1: Parameters used for the stereo PIV evaluation.

Parameter (PIV)	**setting**	**Parameter (validation)**	**setting**
dewarped resolution	4096 px x 2048 px (scale ≈ 0.5 mm/px)	max. displacement	9 px
pre-processing	3 x 3 Gaussian low pass	min. signal-to-noise ratio	5.0
interrogation method	multi-grid stating with (256 px)² windows	min. correlation coefficient	0.2
final window size	128 px x 96 px (overlap 50 %)	max. reconstruction residuum	1.0 px
time delay	100 ms		

Figure 3 displays an exemplary time series of the area-averaged vertical velocity component $\langle u_z \rangle$ measured at h_{LS} = 17 mm. In this measurement, which records the start of the ventilation system, one would expect a constant vertical velocity after an initial rise. However, the mean vertical velocity decreases again, after reaching a maximum after a few seconds.

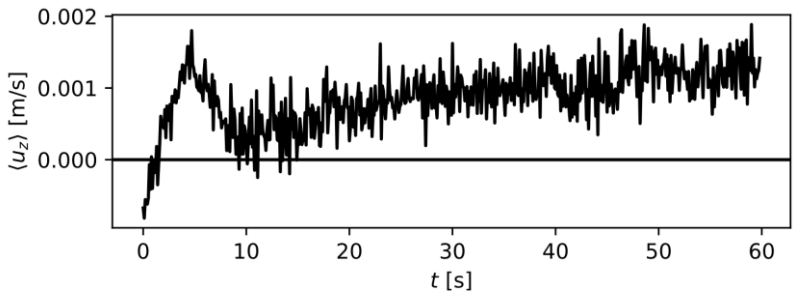

Fig. 3: Time series of the area-averaged vertical velocity component $\langle u_z \rangle$ measured at a height of 17 mm over the mattress after the onset of the ventilation unit (t = 0 s).

GALA e.V., Karlsruhe, Germany, ISBN 978-3-9816764-8-8

For a more detailed view on this issue three instantaneous velocity fields at 4, 10 and 20 s are shown in Figure 4. For t = 4 s, positive (upwelling) vertical velocities were detected for the largest parts within of the mattress perimeter, marked by the rectangle. This field further reveals elevated velocities (≈ 4 mm/s) in the head and leg region compared to the lower upwelling velocities at central y-positions. In the subsequent time steps these velocity magnitudes were no longer reached, despite the ventilation unit operating constantly.

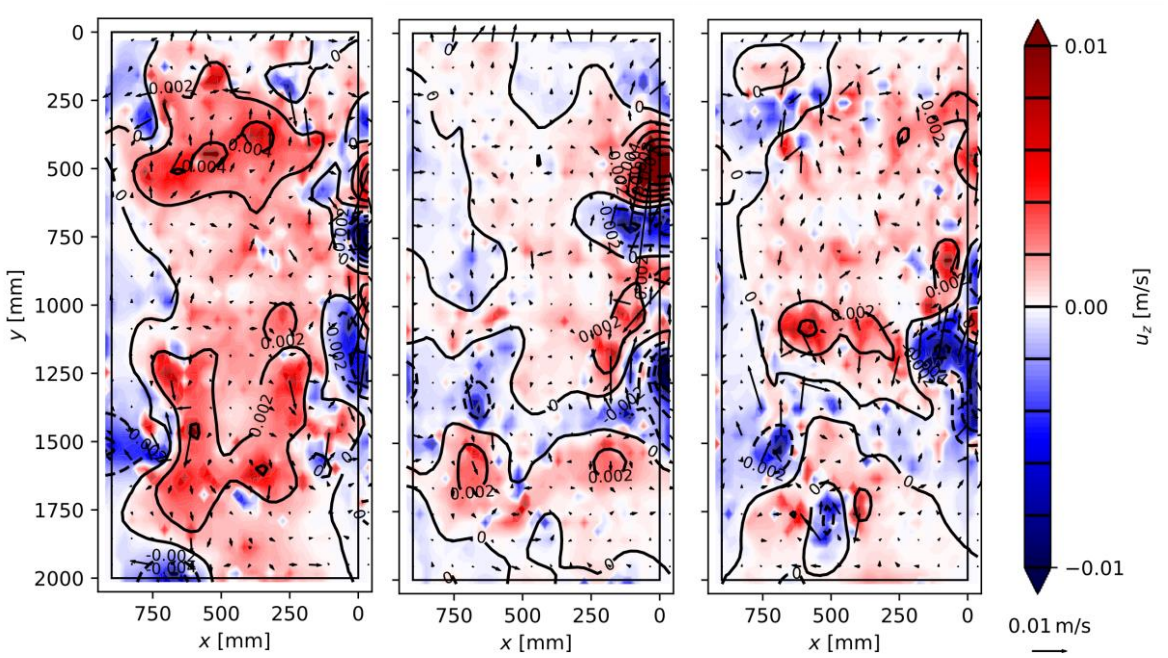

Fig. 4: Exemplary instantaneous PIV velocity fields for 4, 10 and 20 s (left to right). The in-plane velocity is shown by arrows. The vertical velocity component is indicated through color-coding as well as smoothed iso-lines.

This hints at the issue that the contrast between aerosol-rich and aerosol-free swathes was only strong enough to dominate the PIV correlation just after they appear (4-6 s). For the remaining time, the evaluation algorithm correlates on the textile structures of the mattress cover, which cannot be masked without defeating the function of the mattress. This becomes evident by analyzing the correlation plane of a sample at x ≈ 550 mm and y ≈ 620 mm, shown in Figure 5. There, the repeating patterns within the correlation planes indicates an interference of the cover's structure. This effect shifts the correlation peaks towards zeros, leading to smaller displacement vectors and an underestimation of the velocities.

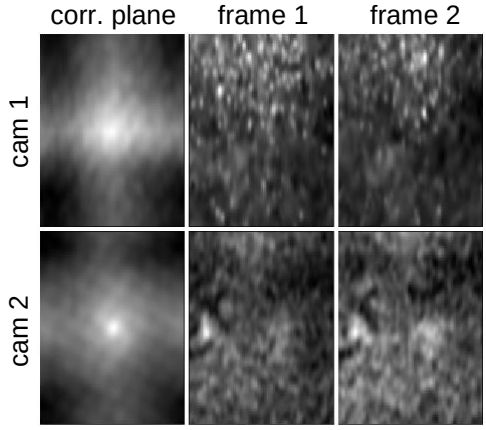

Fig. 5: Correlations planes (left) and correlated frames (right) for an exemplary interrogation window at x ≈ 550 mm and y ≈ 620 mm.

GALA e.V., Karlsruhe, Germany, ISBN 978-3-9816764-8-8

Transit time method

To overcome this issue, a robust method, that depends on the transit time of the aerosol-free air through the different light-sheet planes, was developed. For this measurement technique, the time series of each pixel's gray value, displayed by the in black curve in Figure 6a), is analyzed. For that, the raw images were scaled down by binning 8x8 pixels in order to reduce noise and computing time. Since the resulting time series were still too noisy, a band filter is applied by calculating the difference (green) between two Gaussian filtered signals (blue and orange) with different kernel widths (6 s and 1 s). Thereby, both the short-term fluctuations (< 1 s) of the laser intensity and the slow overall decreasing seeding density (> 6 s) were filtered out.
To determine the passing time of the aerosol-free air, the minima and the falling inflection points of the difference time series can be used. While the global minimum is reliably associated with the aerosol-free air, it may be shifted to later times depending on the width of the trough. In contrast, the falling inflection point indicates the arrival of the aerosol-free air. To determine this inflection point, the 2nd derivative (red) is used. However, its curve shows multiple other sign changes in the course of the time series.

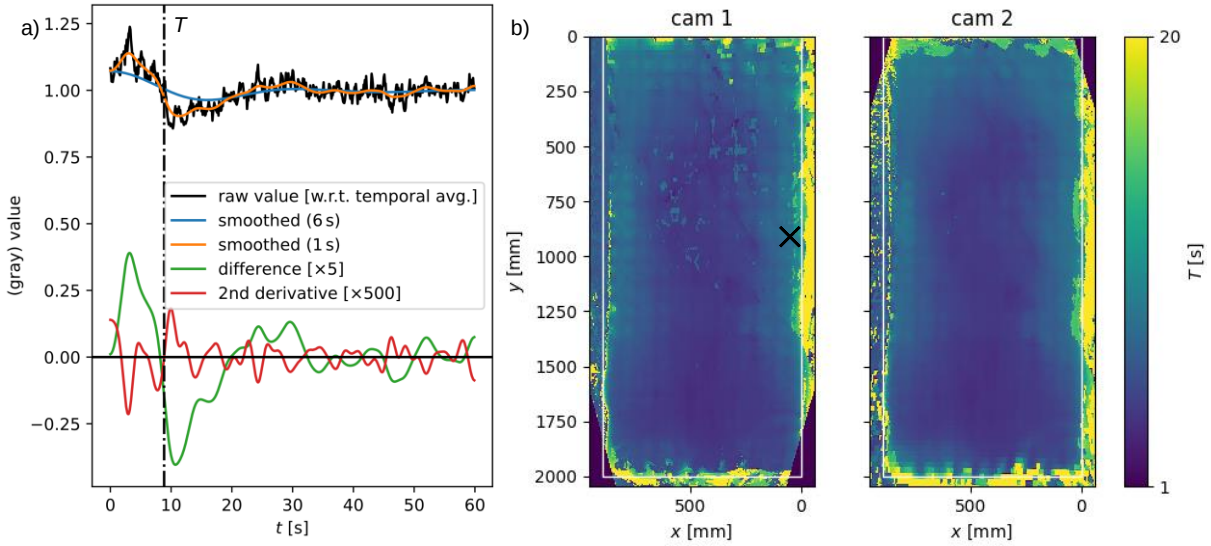

Fig. 6: a) Sample time series of gray values at the position marked with a black cross in b) and curves derived from it. b) Dewarped fields of the calculated transit times T of both cameras. The projected mattress perimeter is marked as white rectangle.

To combine the advantages of the two approaches, the time T, when the aerosol-free air passes the light sheet, is determined by the latest falling inflection point before the global minimum of the difference time series occurs. It is marked by a dash-dotted line in Figure 6a).
Complete dewarped fields of the so determined transit times are displayed in Figure 6b) for both cameras and a measurement case of the blank mattress at h_{LS} = 17 mm. The plots show that the results for both cameras are very similar, which proves the robustness of the method. However, this method is also sensitive enough to detect the structures of the foam under the mattress cover that affect the airflow distribution.
The transit times measured for a single plane already allow an estimation of the velocities. But a single measurement cannot account for the momentum transfer interactions within the mattress, which might lead to delayed outflow at the head end. Since this delay is difficult to estimate, the vertical velocity should be determined by the transit times, T_1 and T_2, for two light-sheet planes with different heights, h_{LS1} and h_{LS2}. Assuming negligible horizontal velocity components, the estimated vertical velocity u_z is determined as follows:

GALA e.V., Karlsruhe, Germany, ISBN 978-3-9816764-8-8

$$u_z = \frac{h_{LS2} - h_{LS1}}{T_2 - T_1}$$

To enable a subtraction of transit times, appropriate calibrations of the individual light-sheet planes are required as for the dewarping of the PIV. Further, multiple repetitions of the measurement of the same case should produce results with a reasonable consistency. With the objective to quantify the reproducibility, the fields of the mean value ($\mu(T)$) and relative standard deviation ($\sigma(T)/\mu(T)$) for 6 measurements (3 repetitions and 2 cameras) for the case of the blank mattress and h_{LS} = 17 mm are depicted in Figure 7. The contour maps show, that sufficiently low relative standard deviations ($\sigma(T)/\mu(T) < 0.1$) are reached with the exception of regions close to the projected perimeter (red) of the mattress.

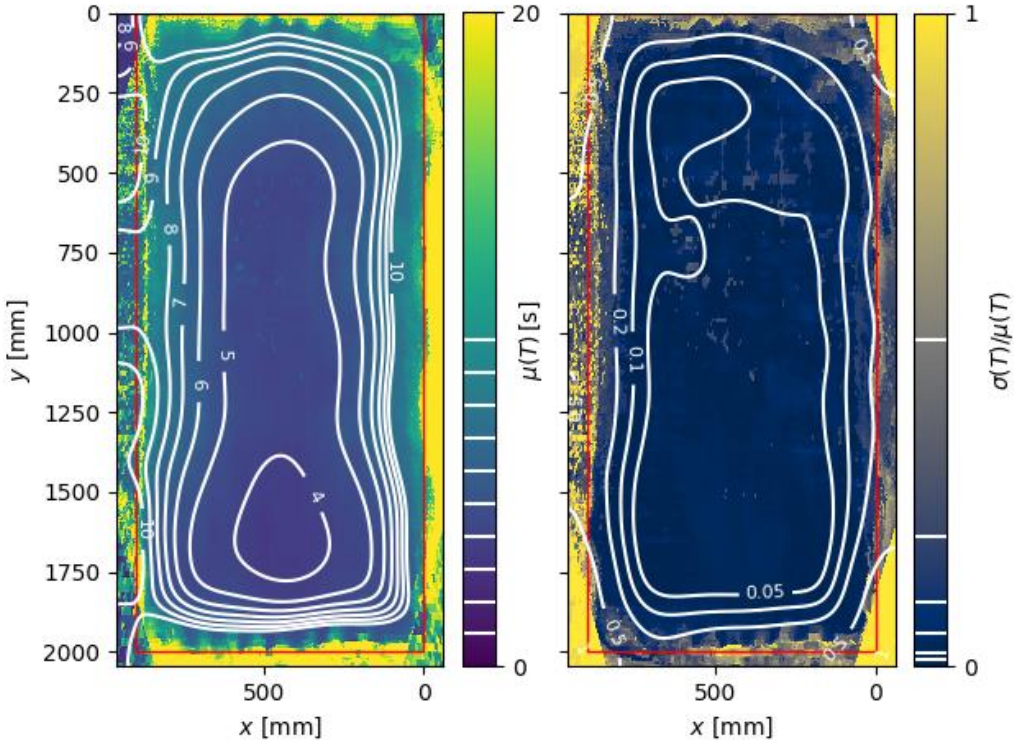

Fig. 7: Field of the transit time averaged over multiple measurements (left) and the field of the respective relative standard deviation (right) with smoothed iso-lines, respectively.

Homogeneity analysis

To evaluate the airflow homogeneity, the transit times T_1 and T_2 were measured in the light sheet planes h_{LS1} = 17 mm and h_{LS2} = 41 mm. In a first case, the transit times were used to calculated the vertical velocities over the mattress with the ventilation unit operating at maximum power. That is shown in Figure 8.

GALA e.V., Karlsruhe, Germany, ISBN 978-3-9816764-8-8

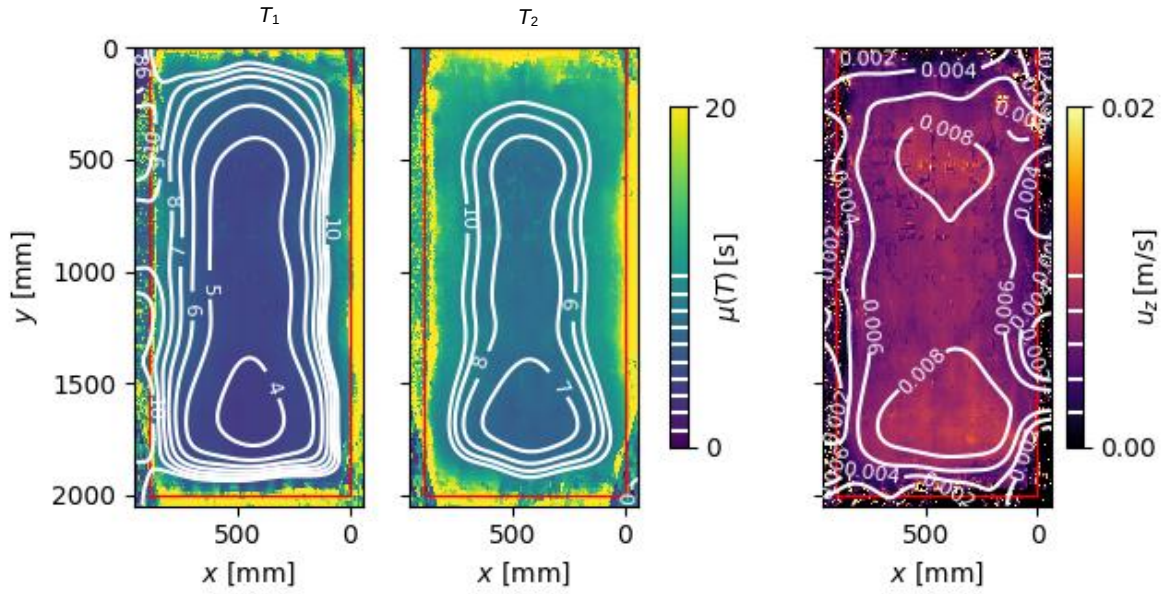

Fig. 8: Mean transit time fields of the two light sheet planes (left) and the field of the resulting velocities (right) for the case of the unloaded mattress with smoothed iso-lines, respectively.

The two transit time plots of the different light sheet planes on the left side indicate the expected shifts to longer transit times for the higher light sheet plane. The velocity plot on the right side of Figure 8 confirms, that the airflow is well-distributed throughout the whole surface of the mattress. The velocity is estimated to be 6-8 mm/s for most regions. Furthermore, two regions with elevated velocities of 8-10 mm/s near the head and foot end become apparent.

As a next step, the method was used, to detect changes in the airflow distribution, when regions of the mattress are under load. Therefore, a generic load of two 10 kg weights was positioned on a 2 mm polyethylene sheet (0.5 x 0.25 m²) to simulate the influence of body weight without obstructing larger areas of the mattress. Figure 9 depicts the load's placement in the center of the mattress, where the highest loads are expected according to Low et al. 2017.

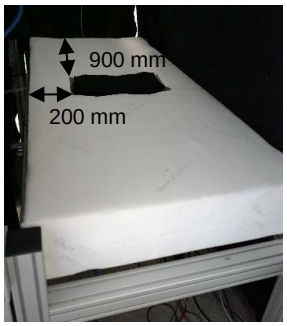

Fig. 9: Generic test load placed in the center of the mattress, viewed from the head end.

The results of the measurements for respective case are displayed in Figure 10. The two transit time plots on the left already reveal that the load blocks the air flow, since the transit times are strongly elevated in the region of the load marked with the small red rectangle. In addition, the velocity plot on the right shows that the load creates a stagnation region extending towards the foot end, in which the vertical velocities rise up to multiples of 10 mm/s. Accordingly, the regions extending from the load towards the head end exhibit lower velocities as in the unloaded case. However, the iso-lines indicate that there is still an airflow with approximately 6 mm/s. This proves that the foam structure is strong enough to keep the ventilation channels open under load, so that the airflow can be distributed past the loads.

GALA e.V., Karlsruhe, Germany, ISBN 978-3-9816764-8-8

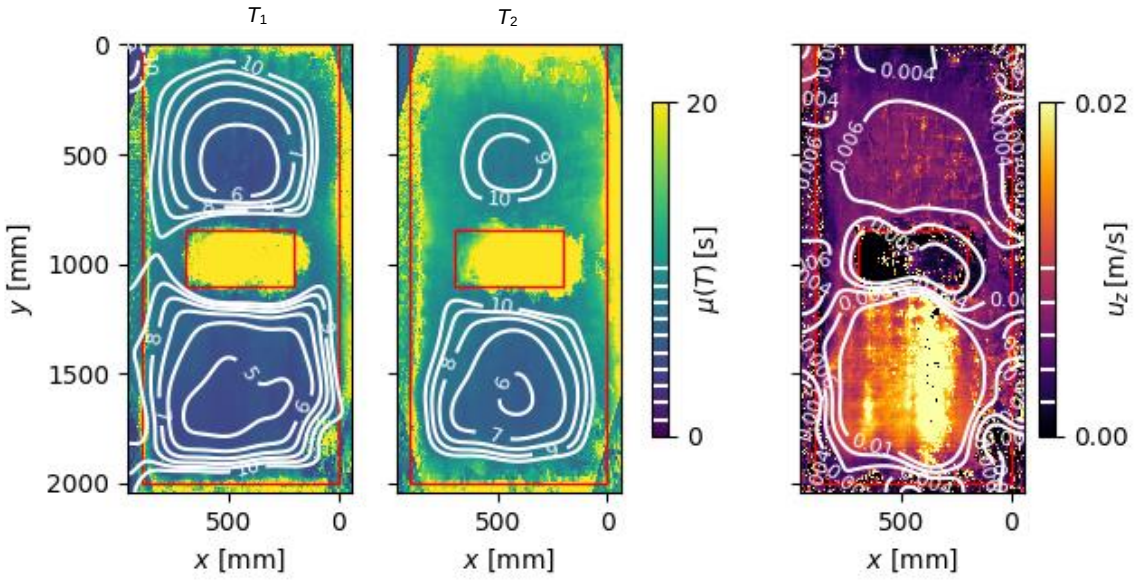

Fig. 8: Mean transit time fields of the two light sheet planes (left) and the field of the resulting velocities (right) for the case of the loaded mattress with smoothed iso-lines, respectively.

Conclusion and Outlook

The velocity evaluations with stereo PIV have shown, that it is possible to reconstruct velocity vectors from the correlation of aerosol-rich and aerosol-free regions, but these calculations underestimate the velocity due to the structure of the mattress cover, which affects the correlation and cannot be corrected sufficiently.
Therefore, a transit time method was developed and applied to calculate the mattress air-outflow velocity and its spatial distribution. It was found that a homogeneous velocity distribution exists in the unloaded test case. However, a stagnation area with elevated velocities forms, when the mattress is loaded. In this case, the channel structures of the mattress are nonetheless able to supply regions behind the load with fresh air.
Overall, the transit time method proved to be suitable to measure these slow flows and will be applied to further test cases. Moreover, this method could also be applied to investigate other low momentum air outlets of air-conditioning systems.

Acknowledgement

The presented work has been supported by the grant “KliMat” of the European Regional Development Fund (ERDF) and the federal state of Lower Saxony. The authors would like to thank Nbank for its support.

Literature

Techniker Krankenkasse (Ed.), **2017**: “Schlaf gut, Deutschland – TK-Schlafstudie 2017”, pp. 25-29.
Low, F.-Z., Chua, M.C.-H., Lim, P.-Y., and Yeow, C.-H., 2017: “Effects of Mattress Material on Body Pressure Profiles in Different Sleeping Postures” J. Chiropr. Med. 16:1–9
Raffel, M., Kähler, C.J., Willert, C.E., Wereley, S.T., Scarano, F., Kompenhans, J., 2018: "Particle Image Velocimetry: A Practical Guide", pp.49–60

GALA e.V., Karlsruhe, Germany, ISBN 978-3-9816764-8-8